Numerical investigation of auto-ignition characteristics in micro-structured catalytic honeycomb reactor for CH_4-air and CH_4-H_2-air mixtures

By:
H. Kayed[a], A. Mohamed[a], M. Yehia[a], M. A. Nemitallah[b,*], and M. A. Habib[b]
[a] Mechanical Power Department, Cairo University, Giza, Egypt
[b] TIC in CCS and Mechanical Engineering Department, Faculty of Engineering, KFUPM, Dhahran 31261, Saudi Arabia

Abstract
Stable ranges of auto-ignition for the micro-combustion of CH_4 and CH_4-H_2 mixtures are identified numerically in a platinum-coated micro catalytic honeycomb reactor. Steady and transient simulations under pseudo-auto-thermal conditions were performed to investigate the coupling phenomenon between combustion and heat transfer in such micro burner using ANSYS 17.2 coupled with a detailed CHEMKIN reaction mechanism. The model was validated utilizing the available data in the literature on a similar micro reactor, and the results showed good agreements. A certain amount of heat is furnished from outside at constant temperature from an external electric furnace to investigate the variations of localized self-ignition temperature while changing the flow rate and mixture strength. It was found that the ignition temperature for CH_4-air mixtures is not affected by the mass flow rate. However, the ignition temperature of CH_4-H_2 air mixtures decreases while increasing the flow rate. Effect of equivalence ratio was studied to demonstrate the variations of flammability limits of the present micro-reactor. The equivalence ratio required for auto-ignition of CH_4-air mixtures was found to be in the range from 0.4 up to 0.85 at a flow rate of 9.5 g/s. The reaction front moved from upstream to downstream under transient conditions matching with the reported experimental behavior in the literature.

Keywords: Auto-ignition; Catalytic combustion; CHEMKIN; Hydrogen-enrichment; CFD modelling; Micro-burner.
*** *Corresponding author:*** M. A. Nemitallah, E-Mail: medhatahmed@kfupm.edu.sa, Tel: +966138604959.
Conflict of interest statement: On behalf of all authors, the corresponding author states that there is no conflict of interest.

Nomenclature

Mix1	Mixture 1
Mix2	Mixture 2
u	Axial velocity of the gas
$\dot{S}_k$	Heterogeneous molar production rate of kth species
A_c	Cross sectional (flow) area
$a_{i,m}$	Effective internal surface area per unit length
P	Absolute pressure
F	Drag force exerted on the gas by the tube wall
h_k	Specific enthalpy of species k
Y_k	Gas-phase species mass fraction
T	Absolute gas temperature
$\overline{c_p}$	Mean heat capacity per unit mass of the gas`
Q_e	Heat flux
Q_e	
a_e	Heat flux surface area per unit length
T_s	Surface temperature
D_k	Species diffusion coefficient
$\nu_{k,m}$,$\nu'_{s,m}$	Stoichiometric coefficients of reactions
A	Collision factor
E	Activation energy
$S_{0,m}$	Sticking coefficient
X_k	Molar concentration of surface species k
K_g	Total number of gaseous species
M_s	Total number of surface species
W_k	Gas-phase species molecular weight
z, y, x	streamwise, transverse, and lateral physical coordinates
MIT	Minimum Ignition Temperature (˚C)
Slph	Standard litre per hour (L/hr)
AFT	Adiabatic Flame Temperature (˚C)
MFT	Maximum Flame Temperature (˚C)

Greek symbols

Φ	Equivalence ratio
θ_s	Surface species coverage
Γ	Surface site density
λ_s	Surface thermal conductivity

X_s	Molar concentration of species S	λ_g	Thermal conductivity of gas
$K_{f,m}$	Arrhenius rate of the mth heterogeneous reaction	μ	Viscosity
$\mu_{s,m}$, $\varepsilon_{s,m}$	Coverage dependence parameters	ρ	Density
R	Universal gas constant	τ	Reactor residence time

Subscripts

k, s	Indices for gas-phase and surface species
G	Gas

1. Introduction

Recent Nano technology progression contributes effectively in minimization of micro electromechanical devices (MEMS). The need for compact, long lifetime and instantly rechargeable power supplies became necessity. So, increasing the operational lifetime of these micro-power generators requires using fuels with high power densities [1,2]. Thus, micro-scale combustion receives promising interest in development of MEMS. As the combustor size is reduced, the combustor surface to volume ratio increases, the time scale of thermal diffusion in solid phase becomes comparable to the time scale of combustion and the flame temperature begins to couple with the temperature of the structure. Thus, leading to strong thermal and chemical couplings between flame, flame-solid interface, and combustor structure establishing multiple flame regimes, in which normal and weak flames may coexist. With the coupling of wall heat loss and auto-ignition at isolated hot spots, isolated flame cells as well as steady/unsteady flame streets can be observed [3-5]. Daou et al. [6,7] studied the effect of flow velocity, Lewis number, and channel width on the flame propagation limit. The results showed that the near wall-flame quenching and flame curvature plays a key role in flame ignition and extinction. Ju and Xu [8] studied the effect of heat loss including the heat transfer in the solid phase and the coupling of flames. The results showed that the flame-wall thermal coupling expands the quenching limit and lead to a new flame regime extending the conventional flammability limit. As a matter of fact, the ignition time becomes shorter when the wall temperature increases. Weak flames or flameless combustion can also be observed. When the ignition time approaches the flow residence time and the combustor size is close to the quenching limit, flame instability via flame extinction and re-ignition takes place. Jackson et al. [9] performed numerical work at fixed wall temperature condition to investigate the physics behind the flame instabilities. The results showed that re-ignition and pulsating flames expressed by violent oscillations occur at a critical value of Damköhler number at various flow rates.

Hua et al. [10] and Norton and Vlachos [11] studied the effects of combustor size and operating conditions, especially heat transfer conditions at chamber wall (e.g. adiabatic wall, with heat loss and heat conduction within the wall), on flame stability. The results indicated that stable combustion may be sustained through increasing the ratio of flow residence time in chamber to chemical reaction time and maintaining proper thermal condition at specific dimensions. Li and Choua [12] studied the effect of combustor size and geometry, inlet velocity profile and slip-wall boundary condition on the flame temperature for premixed CH_4–air mixtures. The results give preference to planar combustor than the cylindrical one over the same velocity range and for the same hydrodynamic diameter. Karagiannidis et al. [13] if combustion could be sustained in small confinements with gaps as small as 0.3 mm. It was also demonstrated for these micro combustors that the effect of slip-wall boundary is negligible when compared to the effects of the bulk velocity and the gases temperature. Tang et al. [14] investigated experimentally the combustion characteristics of three hydrocarbon fuels, namely methane, propane and hydrogen, to compare their flammability limits, quenching diameters and temperature distributions in a micro-planar combustor. The results showed wider stability limits for hydrogen/air flames when compared to propane/air and methane/air flames.

Tang et al. [15] studied the effect of hydrogen addition on combustion characteristics of premixed methane/air within a micro-planar combustor. The results showed that the flame produced by using pure methane is shifted

from the inlet depending on the mass flow rate. In addition, hydrogen addition shifted the flame gradually toward the inlet section. Shabanian and Reza [16] studied the effect of hydrogen feed splitting on combustion stability and outlet gas temperature. The hydrogen is introduced into portions to study its effect on minimizing the deformation of hot entrance spots. The results showed uniform temperature distribution with increased number of feed splitting portions leading to reduced heat losses and increased output temperature. Li and Choua [17] recorded experimentally the transient combustion characteristics in cylindrical micro combustor. The results provide stability maps defined by equivalence ratio and flow velocity for different combustor lengths with the aid of recorded acoustic emissions. The results showed that the backward-facing step combustor design is effective in stabilizing the flame.

The recent dominant trend is directed toward using catalytic combustion to avoid the combustion instabilities under these micro-scale conditions [13,18]. However, many factors limit using the catalytic combustion in power generation including durability and maximum operating temperature. Moreover, catalytic combustion is a water-shed solution to overcome flame instabilities resulting from the heat losses developed in such micro burners. Surface catalytic reactions can be sustained at low temperature and much leaner fuel-air ratios resulting in expanding the flammability limits and having safety privilege. Xu and Ju [19,20] and Aghalayam et al. [21] studied the non-equilibrium effects, via temperature and concentration slips, on the wall and radical quenching in a micro-scale combustor. The results showed that the slip effect influences the catalytic reactions through the dominant effect of both the reaction rate and the diffusion transport leading to propagation of a nonlinear reaction rate distribution at higher Damköhler number. Karagiannidis et al. [13] studied experimentally and numerically the stability limits of heterogeneous/homogeneous combustion for methane-fueled channel-flow catalytic platinum-coated micro reactors. The numerical study was performed using a fully elliptic two-dimensional (2-D) model. An important finding was that the gas-phase chemistry extended the low-velocity stability limits owing to the established strong flames. The high-velocity blowout limits were also extended owing to the heat release originating primarily from the incomplete oxidation of methane.
Catalytic combustion of hydrogen fuel over the catalysts has low activation energy, causing very fast reactions. Hydrogen-air mixtures were found to be self-igniting over platinum wires under fuel-leaner conditions [22]. However, the fuel-richer mixtures ignite at a temperature above room temperature [23]. So, hydrogen is used as exciting assistant enabling micro-scale combustion without ignition source, as it promotes the formation of radicals that attacks CH_4 as well as H_2. Chen and Xu [24] studied numerically the effect of hydrogen addition on the ignition characteristics of propane-air mixtures over platinum-coated micro-channels. The simulation results showed auto ignition of propane-air mixtures with the aid of hydrogen at preheated feed temperature. The results showed that the position of the localized ignition depends on both the equivalence ratio and the wall thermal conductivity. The minimum hydrogen content enabling self-ignition was found to be in the rage from 0.8% to 2.8% depending on the wall conductivity and the inlet velocity bearing in mind the coupling phenomenon between heat and mass transfer in these micro burners. Barbato et al. [25] studied experimentally the auto-ignition of methane and methane–hydrogen mixtures over a Pt-$LaMnO_3$ catalytic honeycomb by varying the gas flow rate and reactants concentrations and composition. The results demonstrated that the needed heat supply to ignite the combustion can be significantly reduced through hydrogen enrichment of the fuel. Zimont [26] studied analytically the auto ignition characteristics over same reactor, as in Barbato et al. [21], but using the zero-dimensional (0-D) approach developed by Semenov et al. [27] and Zel'dovich et al. [28]. This study introduces operation limits that were not tested in the experiments and provide sensitivity analysis for the variation of each parameter and its effect on the ignition characteristics. The results showed that the quenching temperatures of CH_4 and CH_4/H_2 fuels are similar; however, the self-ignition temperatures for them are totally different. Cimino and Di Benedetto [29] studied the methane transient catalytic combustion showing during start-up and shutdown conditions that the flame front moves from the outlet to the inlet of the reactor and methane-air mixture is converted to CO_2 and H_2O because of specified pre-heating temperature that is neither affected by the flow rate nor the reactor length. Tang et al [30] investigated experimentally and numerically the combustion characteristics of premixed propane/air in micro-planar combustor with and without cross plate. The cross-plate length has considerable effect on the flame shape and temperature distribution of the external wall. It improves the heat transfer between mixture and combustor inner wall with at least 90 K temperature rise of external wall when compared to the straight-channel combustor. The flame stability is

enhanced because of using dimensionless plate length of 5/9 for the new combustor; the blowout limit can be raised by 0.4 m/s at equivalence ratio of 0.7.

In the present study, computational fluid dynamics (CFD) study is performed to validate the auto ignition behavior of CH_4-Air mixtures with and without hydrogen addition over a 3-D micro catalytic honeycomb reactor (Unlike the 0-D approach used by Zimont [26]). The aim of the present study is to demonstrate the effects of flow rate, equivalence ratio and reactants composition on controlling the minimum ignition temperature at steady-state conditions to maintain stable operation of the reactor. The role of H_2 addition is analyzed in relation with the total flow rate. Transient simulations are also performed considering 3-D description of gas and solid phases, heat conduction across the solid wall, and gas and surface reactions in the reactor to determine the positions of flame during the start-up conditions.

2. Computational Scheme

2.1 Physical model of the micro-reactor

A schematic configuration of the catalytic honeycomb reactor considering mixture inlet, preheating, and exhaust sections is shown in Fig.1-a. The honeycomb monolith is wrapped in an alumina blanket to avoid heat losses, and the bypass of reacting flow is then inserted in a quartz tube positioned in a tubular electric furnace. The designed domain is identical to the lab-scale reactor built by Barbato et al. [25]. The electric furnace enables a step control on the surface temperature as it is considered as the minimum ignition temperature. This temperature not only responsible for preheating the mixture introduced, but also provides the heat needed to sustain combustion overcoming high heat losses resulted from the high surface to volume ratio of such micro reactor.

The micro-reactor is modeled as a honeycomb cut in shape of a disk of 17 mm diameter and 12 mm length as shown in Fig.1-b. The honeycomb is 900 cpsi (cell per square inch) with solid wall thickness of 0.051 mm. Substitution of these values in equations 1 and 2 results in 317 cells with cell diameter of 0.85 mm and the ratio of volume of catalyst to cavities in the honeycomb is about 27.2% [35].

$$D_{cell} = 25.4\left((cpsi)^{-\frac{1}{2}} - \frac{t_w}{1000}\right) \qquad mm \qquad (1)$$

$$A_{flow} = \frac{cpsi}{(2.54)^2}\frac{\pi}{4}D_r^2 D_{cell}^2 \qquad mm^2 \qquad (2)$$

Platinum catalyst with surface site density of 2.7×10^{-8} kgmol/m^2 and 1.1 g weight is coated on the inner surfaces of the reactor cells.

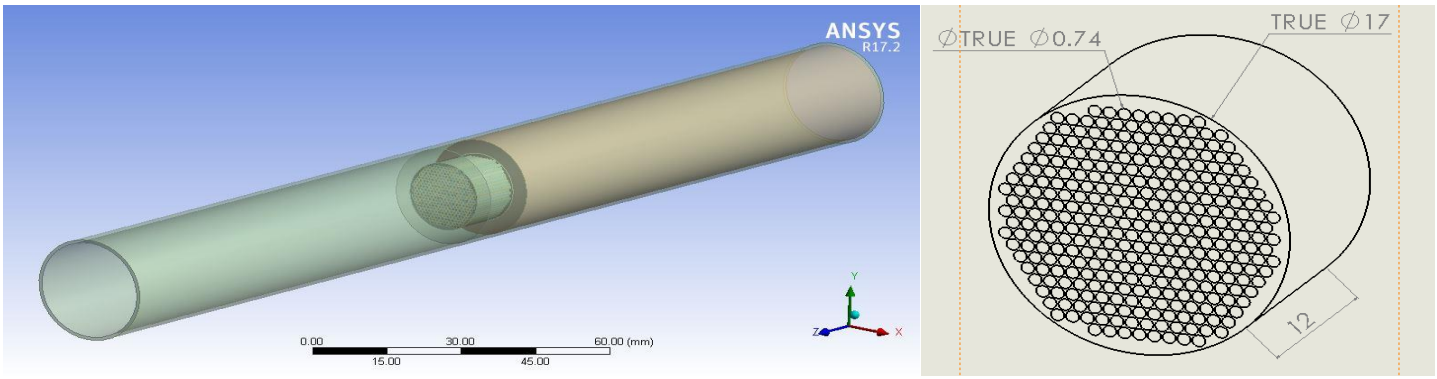

(a) (b)

Fig.1. Representation of the catalytic honeycomb reactor: (a) Full 3-D representation and (b) honeycomb cut.

Three engineering materials are defined for the quartz tube, alumina blanket and honeycomb monolith zones in order to couple their properties while calculating the heat loss during the combustion process. The engineering properties for these materials are reported in Table 1.

Table 1. Characteristic properties of zone materials.

Material	k ($\frac{W}{m.k}$)	ρ ($\frac{kg}{m3}$)	C_p ($\frac{J}{kg.k}$)	Zone
Quartz Glass	0.71	2500	1045	Quartz tube
Alumina	0.125	64	871	Alumina blanket
Cordierite	2	2600	1464	Honeycomb Monolith

Two different compositions of gas mixtures are examined and fed to the reactor at 40-160 slph at a temperature, which is assumed to be the localized self-ignition temperature. The mixtures, *Mix1* and *Mix2*, are of different compositions, but they are supplied with the same heat input as indicated in Table 2.

Table 2. Characteristics of the considered fuel mixtures in the present study.

	Fuel	
	CH_4	CH_4-H_2
	Mix1	*Mix2*
H_2 (%)	-	2.1
CH_4 (%)	2.8	2.2
O_2 (%)	10	10
N_2 (%)	87.2	85.7
Equivalence ratio (Φ)	0.56	0.54
Input heat flux, kJ N l^{-1} (W/m^2)	0.9	0.9
Thermal power, W	10–35	10–35
Volume flow rate range 11–44.5 cm^3/s		

2.2 Governing equations

Neglecting radiation and body force term, In particular, the basic governing equations concerning the catalytic combustion read:

$$\rho u \frac{dA_c}{dx} + \rho A_c \frac{du}{dx} + u A_c \frac{d\rho}{dx} = \sum_{m=1}^{M} a_{i,m} \sum_{k=1}^{K_g} \dot{S_{k,m}} W_k \qquad (3)$$

Here ρ is the (mass) density and u the axial velocity of the gas, which consists of k_g species. W_k is the molecular weight of species *k*, and $\dot{S}_k$ is the molar production rate of this species by all surface reactions. The quantities A_c and $a_{i,m}$ are the cross sectional (flow) area and the effective internal surface area per unit length of material, respectively, in the reactor. Both A_c and $a_{i,m}$ can change as arbitrary functions of *x*.

The momentum equation for the gas expresses the balance between pressure forces, inertia, viscous drag, and momentum added to the flow by surface reactions. Thus:

$$A_c \frac{dP}{dx} + \rho u A_c \frac{du}{dx} + \frac{dF}{dx} + u \sum_{m=1}^{M} a_{i,m} \sum_{k=1}^{K_g} \dot{S_{k,m}} W_k = 0 \qquad (4)$$

Where *P* is the absolute pressure and *F* is the drag force exerted on the gas by the tube wall. Energy and surface site species equations for the micro-reactor are formulated into equations 5 and 6 respectively as follows;

$$\rho u A_c \left(\sum_{k=1}^{k_g} h_k \frac{dY_k}{dx} + \overline{c_p} \frac{dT}{dx} + u \frac{du}{dx} \right) + \left(\sum_{k=1}^{K_g} h_k Y_k + \frac{1}{2} u^2 \right) \sum_{m=1}^{M} a_{i,m} \sum_{k=1}^{K_g} \dot{S}_{k,m} W_k = a_e Q_e - \sum_{m=1}^{M} a_{i,m} \sum_{k=1}^{K_g} \dot{S}_{k,m} W_k h_k \qquad (5)$$

$$\dot{S}_k = 0 \qquad k = k_s^f, \ldots k_s^l \qquad (6)$$

Where $\dot{S}_{k,m}$ is the heterogeneous production rate that generally depends on the composition of the surface and the gas as well. Assuming that these species are immobile, the steady-state conservation equations are simply stated in equation (6). The surface species conservation equation is applied to every species in each surface phase (*n*) contained on each surface material (*m*).

2.3 Combustion model

In the present work, the combustion of surface honeycomb monolith reactor is modelled using ANSYS CHEMKIN-PRO17.2 package. The elementary heterogeneous kinetics mechanism of Deutschmann et al. [31] was used to predict the combustion process. The model considers 17 gas-phase species (including CH_4 ,CH_3, CH_2,CH,CH_2O, HCO, CO_2,CO ,H_2, H, O_2, O,OH,HO_2, H_2O_2 ,H_2O,N_2) and 11 site species (Pt(S) ,H(S) ,H_2O(S) ,OH(S), CO(S) ,CO_2(S), CH_3(S), CH_2(S), CH(S), C(S), O(S)) with 58 volumetric reactions and 23 surface reactions with surface site density of 2.7×10^{-9} mole/cm^2 during the combustion of CH_4 over Pt catalyst. Both volumetric and surface elementary reaction rates are evaluated through importing reaction mechanisms from CHEMKIN for CH_4 combustion over Pt catalyst including backward reaction, third body efficiencies and coverage-dependent reaction.

2.4 Boundary conditions

The inlet boundary of the reactor is defined as mass flow-inlet and its mass is calculated at the surrounding temperature for different fuel flow rates. A pressure-outlet boundary is used at the exit section of the reactor. At all interfaces between the solid and the fluid phases, coupled heat transfer is performed with no-slip condition governed by equations (7 and 8) [33]:

$$-\lambda_s \frac{\partial T_s}{\partial r} + \sum_{k=1}^{K_j} M_k \dot{S_k} h_k = -\lambda_g \frac{\partial T_g}{\partial r} \qquad (7)$$

$$\dot{S_k} M_k + \rho D_k \frac{\partial Y_k}{\partial r} = 0 \ (k = 1,2, \dots, k_i) \qquad (8)$$

Where $\dot{S_k}$ is define as the heterogeneous production or depletion rate of gaseous/surface species *k*, calculated based on equation (9):

$$\dot{S_k} = \sum_{m=1}^{N_j} k_{f,m} \nu_{k,m} m \prod_{S=1}^{K_i+k_j} [X_s]\, \nu'_{s,m} \left(k = 1,2, \dots, K_i + K_j\right) \qquad (9)$$

Where $\nu_{k,m}$ and $\nu'_{s,m}$ are the stoichiometric coefficients, X_s is the molar concentration of species *S*, $K_{f,m}$ is the Arrhenius rate of the m^{th} heterogeneous reaction calculated as:

$$k_{f,m} = A_m T^{\beta m} \exp\left(\frac{-E}{RT_s}\right) \prod_{S=1}^{k_j} \Theta_s^{\mu_{s,m}} \exp\left(\frac{\varepsilon_{s,m}\, \Theta_s}{RT_s}\right) \qquad (10)$$

Where $\mu_{s,m}$ and $\varepsilon_{s,m}$ are the coverage dependence parameters. However, the rate coefficient, K_{fm}, is calculated for the adsorption reaction by the sticking coefficient, S_0:

$$k_{f,m} = \frac{S_{0,m}}{r^{\tau}} \sqrt{\frac{RT_s}{2\pi M_m}} \qquad (11)$$

The molar concentration of surface species *k*, X_s, is defined by:

$$X_s = r\Theta_s \qquad (12)$$

Where *r* is the surface site density of Pt catalyst with the value of 2.7 x 10^{-9} mole/cm^2, and Θ_s is the coverage fraction calculated by:

$$\frac{d\boldsymbol{\Theta_s}}{dt} = \frac{\boldsymbol{S_s}}{\Gamma} \qquad (13)$$

2.5 Numerical Scheme

The stated geometric parameters are implemented in the honeycomb monolith reactor built-in CHEMKIN program to make full description of the catalytic reactor. The domain with 25.4 mm diameter and 250 mm length combines quartz tube, alumina blanket, honeycomb monolith. This domain is discretized to about a million cells as shown in Fig.2. A grid independence study has been performed to take aside the effect of grid refinement on the calculated results. Local meshing is introduced to refine the honeycomb monolith zone and combustion zone. The cell size varies from 60 μm (inside the reactor) to 6 mm (pre-heating and exhaust gases sections) with an average aspect ratio of 2 and average skewness of 0.28.

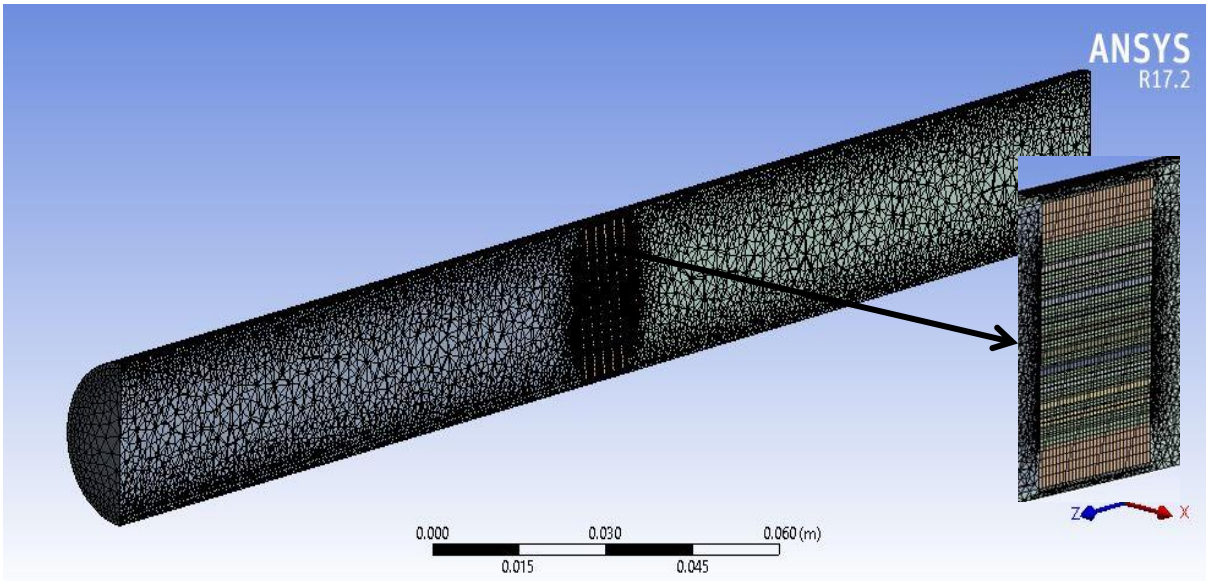

Fig.2. Representative mesh of the developed model.

The surface of the quartz tube is set as constant wall temperature and its temperature is equal to localized self-ignition temperature. Surface reactions are enabled on the inner surfaces of the honeycomb monolith. Under steady-state conditions, laminar model is used to simulate the flow in these honeycomb shape. Finite-rate model is used to simulate the turbulence-chemistry interaction for these micro burners. A detailed mechanism including 23-step-heterogeneous mechanism is adopted together with 58 volumetric reactions to fully simulate the whole chemical process. These reactions are defined by importing CHEMKIN files into FLUENT, and enabling wall surface reactions. A Coupled pressure-velocity solver and pseudo transient mode was enabled to simulate the experimental procedure. For transient simulations, only the honeycomb reactor zone is discretized to 3 million cells controlled by a convenient mesh aspect ratio adopted to catch the localized ignition position. In order to reduce the calculation time, symmetry plane is applied for the full-size model reducing half solution time. The coupling between pressure and velocity is modelled using semi-implicit method for pressure linked equations (SIMPLE) algorithm with double precision solver.

3. Results and Discussion

Results are presented under pseudo-auto-thermal conditions, a certain amount of heat is furnished from outside the reactor, and the heat produced by the reaction should be high enough to maintain the combustion process. In fact, the heat losses are too high to allow thermal auto sustainability with sole reaction heat source; external heat is supplied by maintaining the entire system at a controlled temperature with the electric furnace. That

controlled temperature of the entire external system is defined as inlet mixture temperature, since it can be assumed as the temperature of the entering gas to the reactor after passing through the preheating section. A parametric study is performed on the inlet temperature in order to determine the minimum ignition temperature (*MIT*) for *Mix1* and *Mix2*. Similar experimental conditions of Barbato et al. [25] are taken for the present simulation to validate the model at reference case study (using *Mix1* composition at equivalence ratio of 0.56). Various parametric studies are performed to investigate the effect of equivalence ratio, flow rate and addition of H_2 to CH_4 on ignition characteristics of micro structured catalytic combustor.

3.1 Auto-ignition characteristics

Figure 3 presents the variation of adiabatic flame temperature with minimum ignition temperature for both *Mix1* and *Mix2*. Despite having the same heating input for both mixtures, *Mix2* has slightly higher adiabatic flame temperature than *Mix1* at the same *MIT*. This may be attributed to the existence of considerable percentage of hydrogen in *Mix2*. A great agreement was depicted between the predicted adiabatic flame temperature and measured temperatures done by Boehman [32].

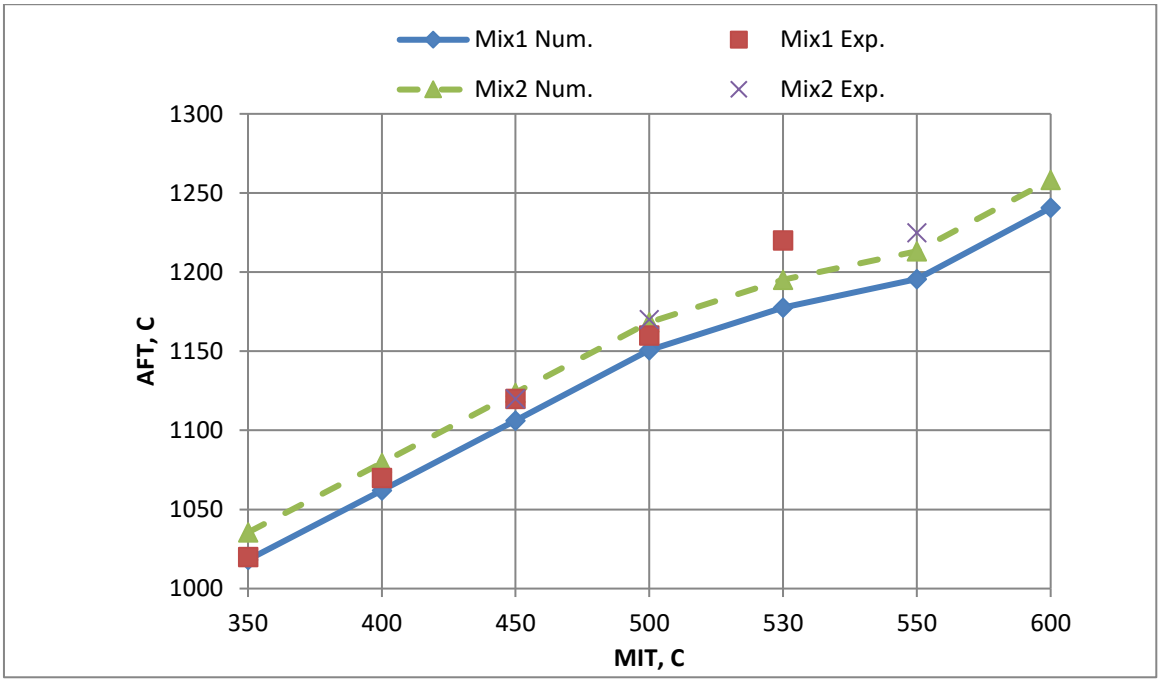

Fig.3. Variation of adiabatic flame temperature versus pre-determined MIT for both *Mix1* and *Mix2*

In order to determine the *MIT* under these operating conditions for this micro-catalytic reactor, the inlet temperature was step-controlled until it triggers auto-ignition and the flame propagates. The furnace continues working to overcome the high heat losses resulting from the high surface-to-volume ratio and to support combustion sustainability. Figure 4 shows the variation of the maximum flame temperature detected along the reactor for different inlet mixture temperatures of *Mix1 and Mix2* at volumetric flow rate of 22 cm^3/s (80 slph). The plot shows that the combustion starts at *MIT* of 500 ˚C and 472 ˚C for *Mix1 and Mix2* respectively, and above these values, the flame temperature does not encounter any significant changes. It is also appeared that addition of H_2 to CH_4 promotes the kinetics mechanism and advancing the auto-ignition temperature around 30 ˚C. A slight difference between MFT and AFT is appeared in ignited region, this difference comes essentially from heat losses across the reactor surface due to high surface/volume ratio; however, other reasons have inconsiderable impact and are ignored.

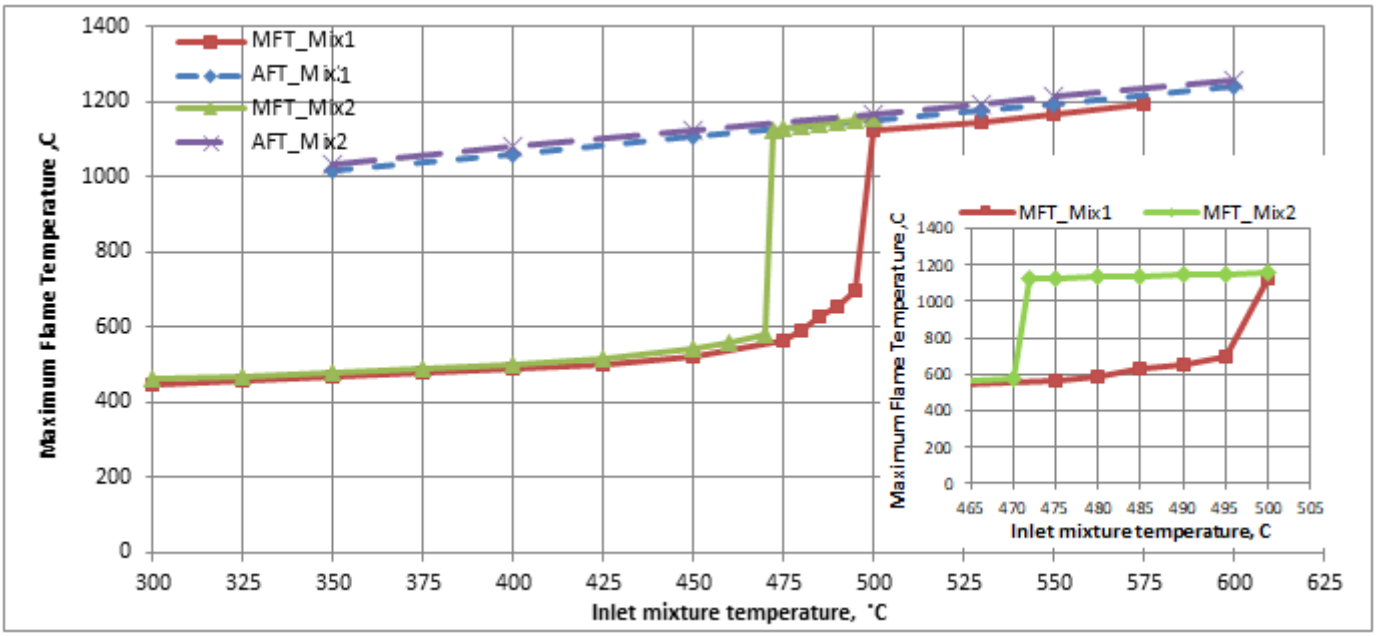

Fig.4. Variation of maximum flame temperature with different inlet mixture temperatures for *Mix1 and Mix2*.

Axial distribution of the flame temperature along the burner is presented in Fig.5 and compared with the experimental data by [25,33] taken at three distinct locations within the reactor (3 mm from the inlet, at the middle and 3 mm before the outlet). The results show that the present numerical model can predict accurately the distribution of the flame temperature. However, the deviations between the experimental data and the numerical results can be explained as result of disregarding the radiation effect in the model or the errors in temperature measurement due to the location of the thermocouple within the reactor. The tip (of 0.5 mm) of the thermocouples in the catalytic honeycomb is placed in close contact with the solid wall of the reactor. Consequently, the gas flow in the measuring channel is strongly reduced due to the presence of the thermocouples and, therefore, the temperature reading in the honeycomb catalyst are believed to be more indicative of the surface temperature although it is a weighted-average with the gas temperature.

The obtained data of *MIT* for similar catalytic micro reactors [29,32] shows good agreement with the present numerical results for the same gas mixture. From figures 4 and 5, a slight deviation between the present work and the experimental data can be attributed to the effect of disregarding radiation and other operational factors including the technique for inlet temperature measurement. Also, the present numerical results of *MIT* are convenient with the measured data by Karagiannidis et al. [13] at pressure of 1 bar. However, large deviation appears at elevated pressures by virtue of reactivity of both catalytic and gaseous pathways at these elevated pressures (up to 16 bar).

The weighted-average overall heat transfer coefficient on the outer wall was predetermined and was found to be 17 $W/m^2/k$. This value is different from that obtained theoretically by Zimont [26] which is localized value of 48.6 $W/m^2/k$. In order to predict the auto-ignition characteristics, the heat produced during the combustion process is investigated and presented in figures 6 and 7. The heat production rate is categorized into two main parts; the surface heat production rate and the volumetric heat production rate. The analysis demonstrates the major role of catalytic surface heat production rate to enhance the activation energy and initiate the combustion process. Figure 6 depicts the surface heat production rate profile which has two spikes that advancing the sole spike of volumetric heat production profile. This advancing promotes the activation energy of intermediate species and accelerate the reaction rates of the kinetics mechanism. Locations of both surface and volumetric heat production rates can be inferred from the distributions of species concentrations along the reactor as shown in Fig.7. The variation detected for H_2 mole fraction and the position of its peak inferred that is strongly affected by surface reactions of the catalyst. However, the impact of volumetric reactions essentially appears on the formation of OH and the location of its peak.

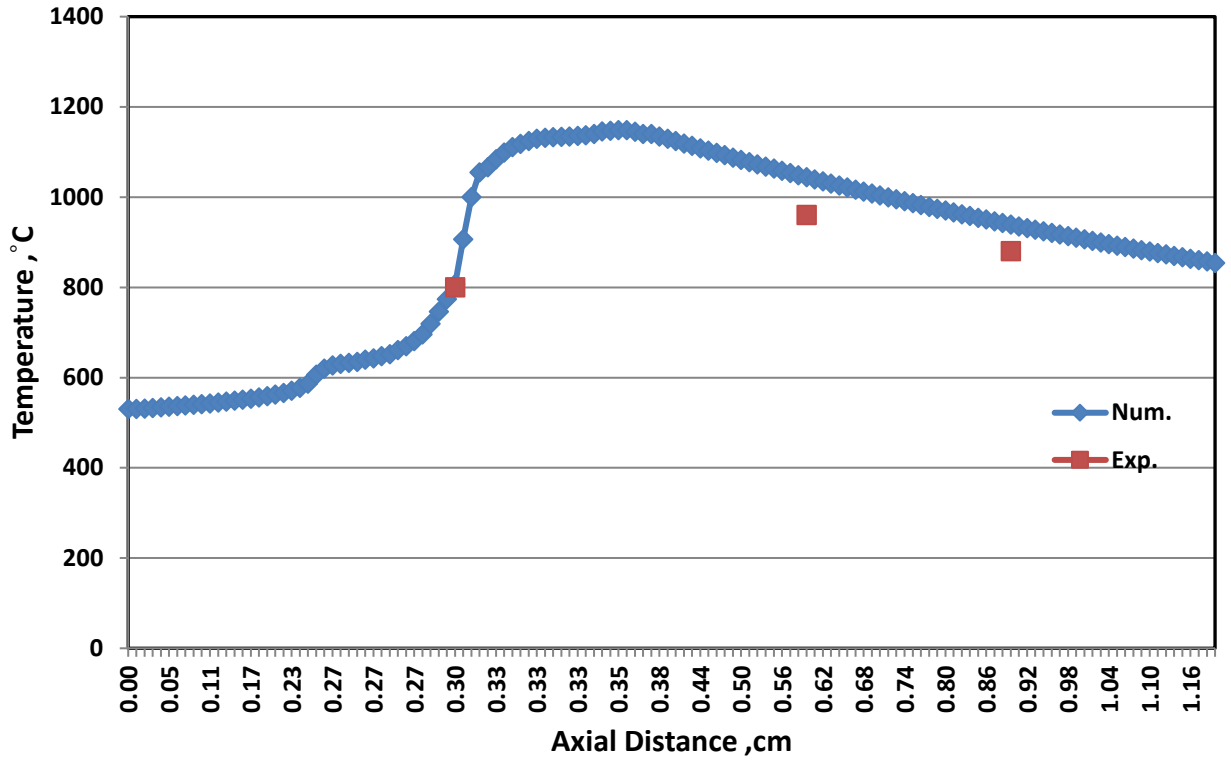

Fig.5. Variation of the flame temperature along the micro reactor in comparison with the experimental data by [25,33].

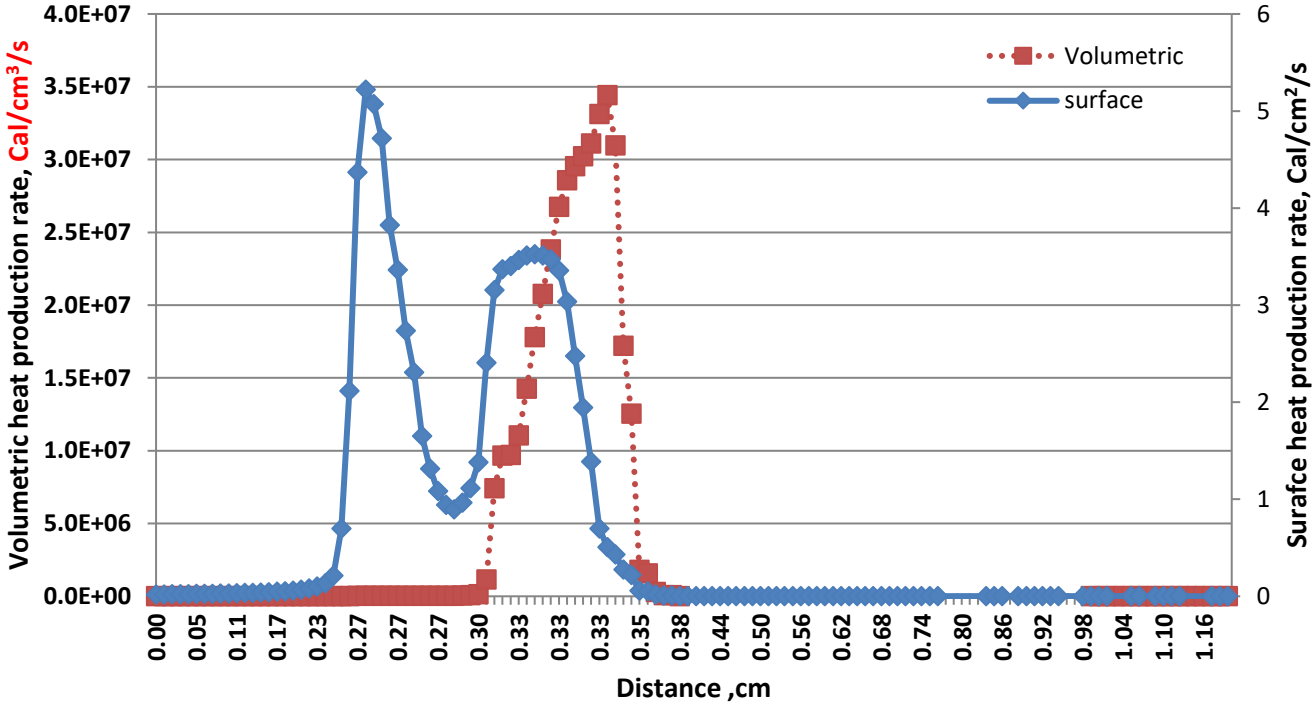

Fig.6. Distributions of the axial surface and volumetric heat production rates (Cal/cm^2/s) along the micro reactor.

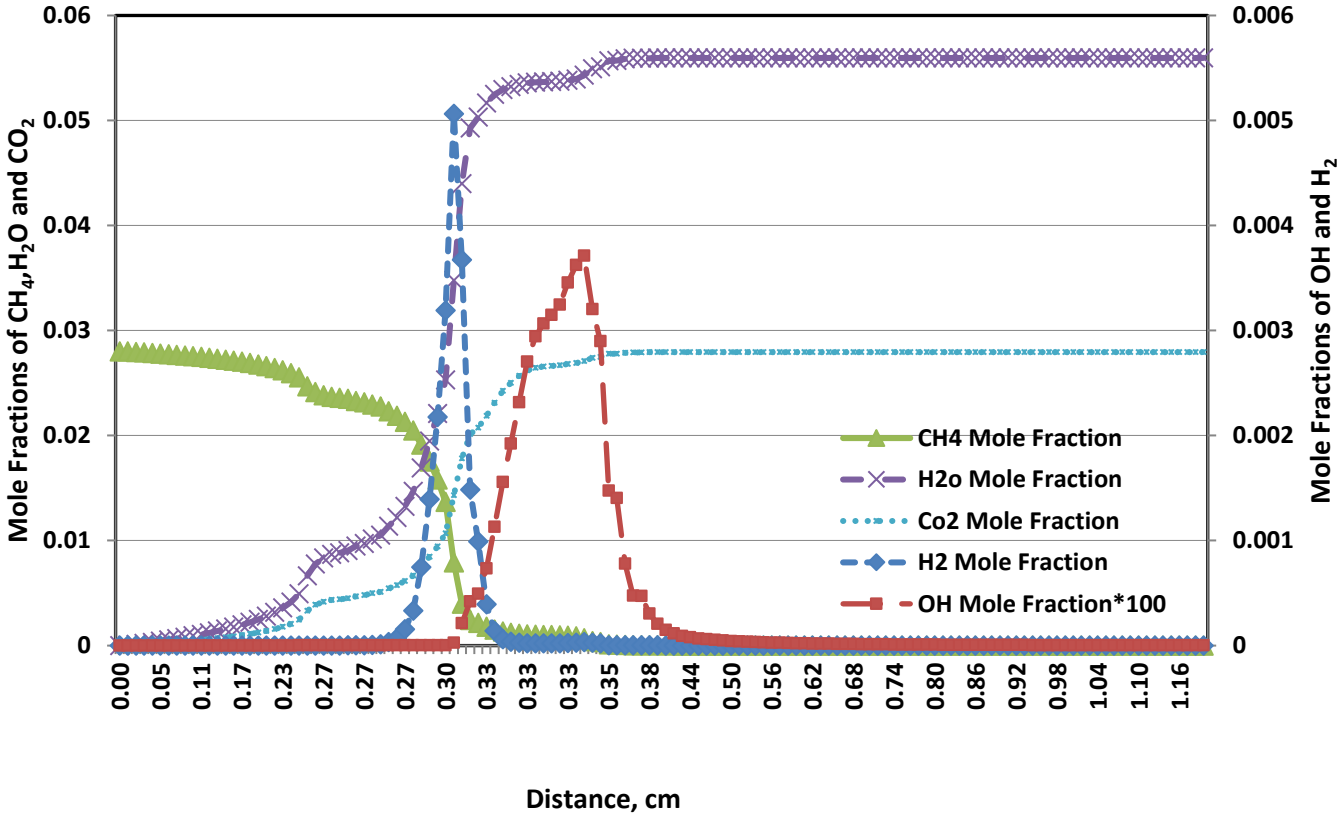

Fig.7. Axial distributions of species mole fractions along the micro reactor.

3.2 Effect of flow rate on auto-ignition characteristics

Effect of the flow rate through the micro reactor on the *MIT* is investigated for *Mix1* and the results are compared with the experimental data [25] as presented in Fig.8. It is shown that the numerical and experimental results of MIT completely conforms at higher flow rates (from 13 mg/s to 28.4 mg/s). There is a considerable deviation between the numerical and experimental results of MIT at lower flow rate (~4.7 mg/s) and this deviation diminishes as long as the flow rate increased. The maximum flame temperature is presented in Fig.9 for different flow rates of *Mix1*. At lower flow rates (4.7 mg/s and 9.5 mg/s), it is shown that the effect of varying flow rate on minimum ignition temperature strongly depends on the balance between volumetric heat generation volumetric heat losses. Conversely, this effect vanishes for higher flow rates (23.6 mg/s and 28.4 mg/s), where the minimum ignition temperature are kept constant.

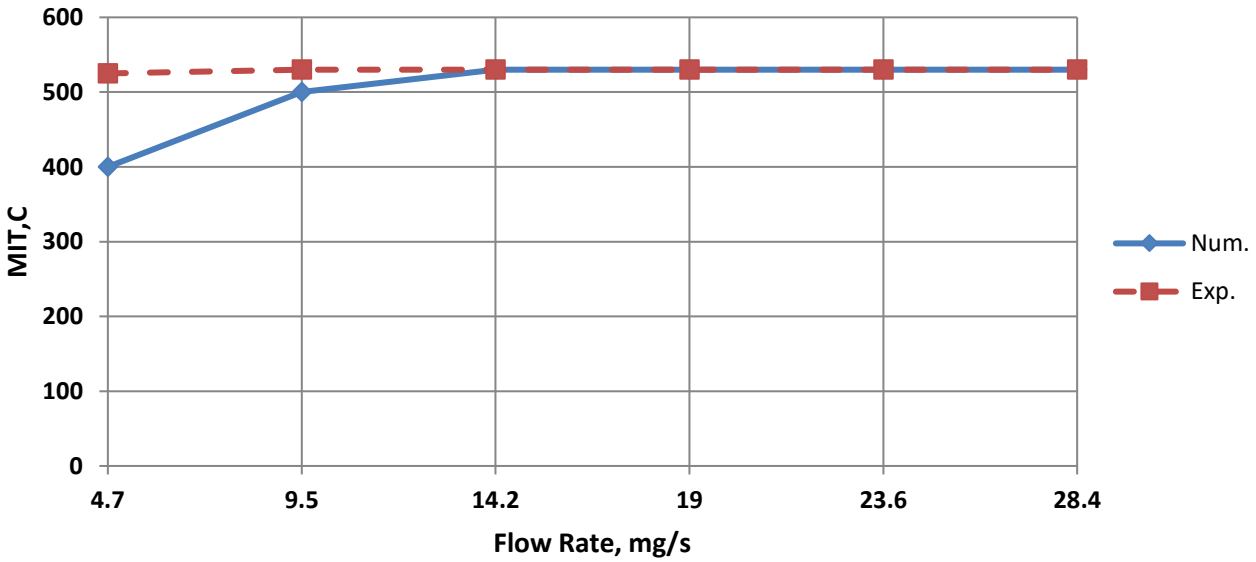

Fig.8. Effect of flow rate of *Mix1* on the *MIT* and comparison with the experimental data by [25].

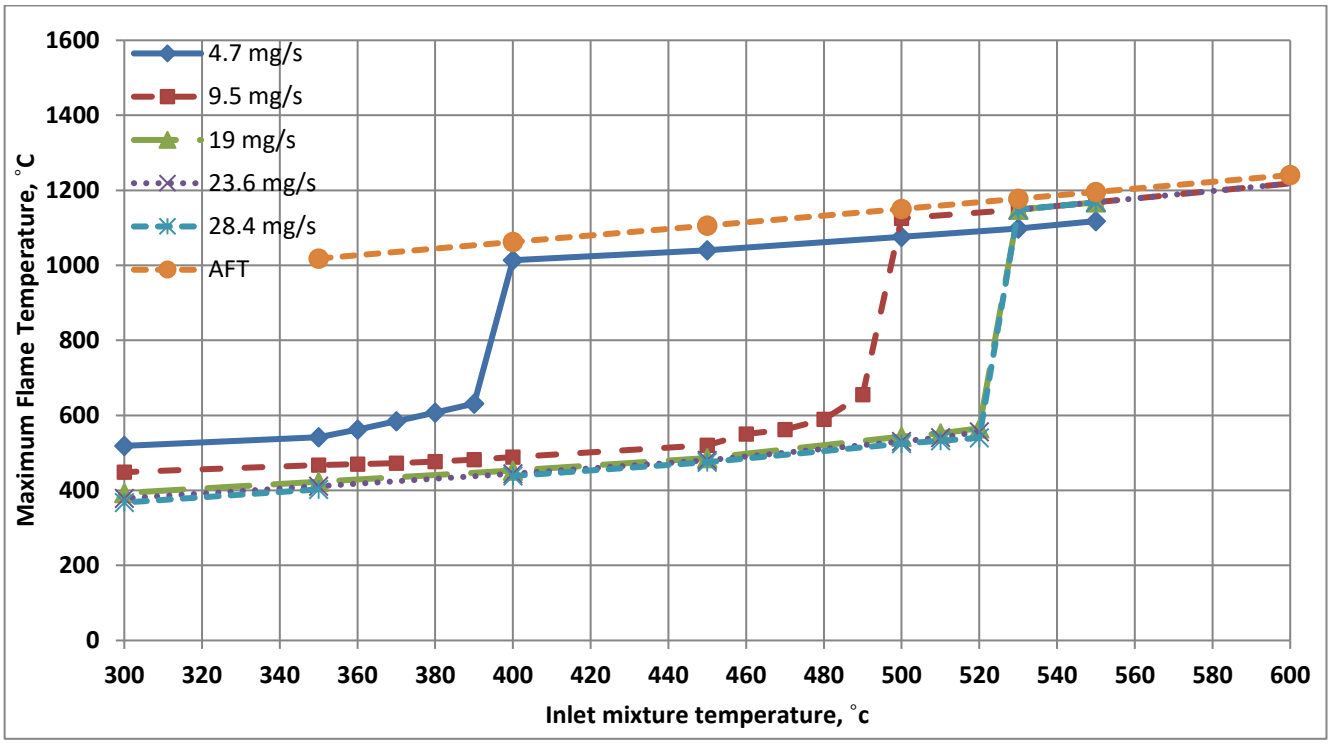

Fig.9. Variation of the maximum flame temperature versus inlet mixture temperature at different flow rates for *Mix1*.

Figure 10 shows the flammable range of equivalence ratios required for methane-combustion in the micro-catalytic combustor at flow rate of 9.5 g/s. It presents the occurrence of flammability limits in lean mixture condition ranged from 0.45 to 0.75. The results indicate new operating limits for methane-combustion over micro catalytic reactors that were not reported experimentally before. This range of equivalence ratio shows great coincidence to the obtained experimental data by Dogwiler et al. [33], which guarantee catalytically stabilized combustion (CST) of a lean methane-air mixture at equivalence ratio of 0.4. The results are also matched with the obtained numerical results by Reinke et al. [34].

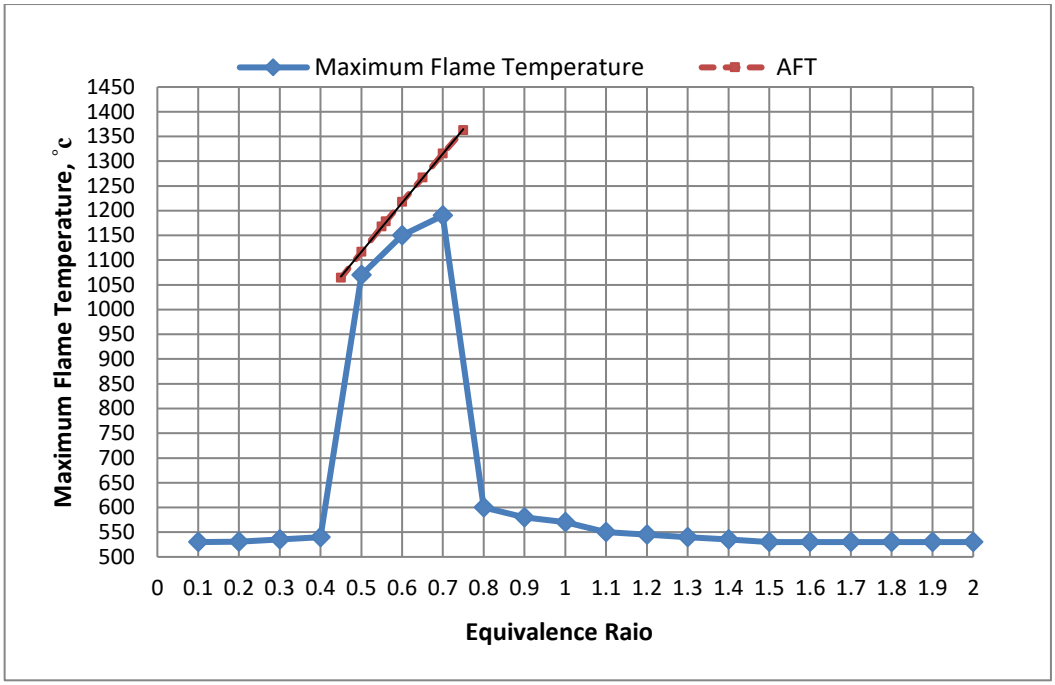

Fig.10. Variation of the maximum flame temperature versus equivalence ratio.

Figure 11 presents the variation of numerical and experimental results [25] of the *MIT* versus flow rate for H_2-CH_4 fuel composition (*Mix2)*. As shown in Figure 11, substituting part of CH_4 with H_2 enhances the fuel reactivity and promotes the mechanism of CH_4 ignition. The change in the heat transfer coefficient for each case is not-considered. The deviation between the numerical and experimental data increases for higher flow rates, and this takes place due to constant heat transfer coefficient assumption which is not the real case.

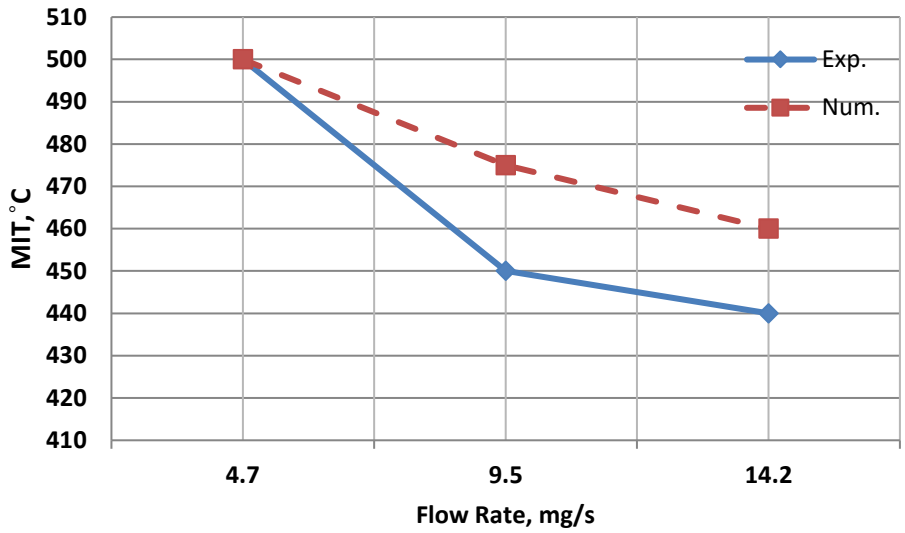

Fig.11. variation of numerical and experimental results [25] of *MIT* versus flow rate for *MIX 2*

Figure 12 presents the steady state contours of temperature along the electric furnace ignited at MIT operated by Barbato et al. [25]. *Mix1* is introduced to preheating section at a temperature of 27 ˚C to gain heat until reaching the *MIT*, which is almost equal to the controlled electric surface temperature. The temperature contours along the tubes of the micro-burners and inside the outer radial micro-tubes are zoomed in Fig.12. The temperature on the outer radial tubes is lower than that on the inner tubes despite having the same Reynolds number (*Re*) due to high heat losses at the outer surface. These temperature contours consolidate the coupling phenomenon between combustion and heat losses inside these micro-reactors. Figure 13 shows the contours of

velocity along the reactor domain. Although the velocity is found to be around 72 cm/s inside the micro-tubes, a small value of *Re* is obtained due to the honeycomb structure where the flow is considered in laminar regime.

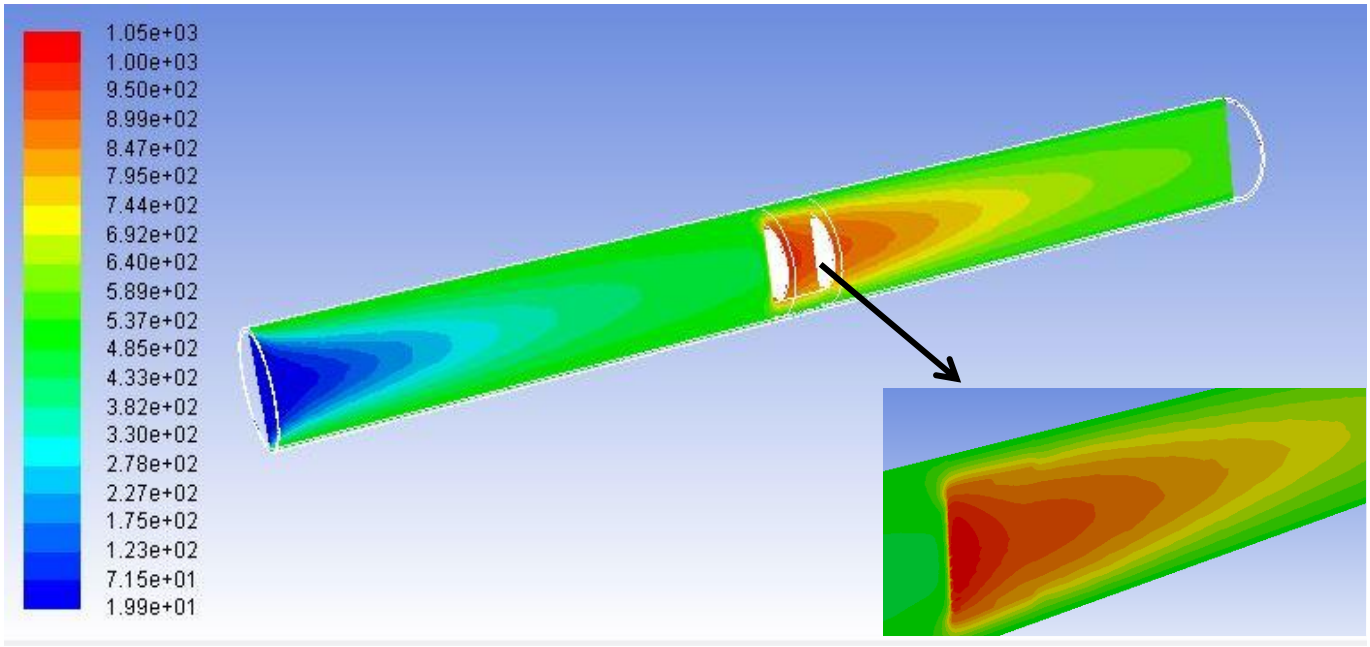

Fig.12. Temperature contours inside the electric furnace domain.

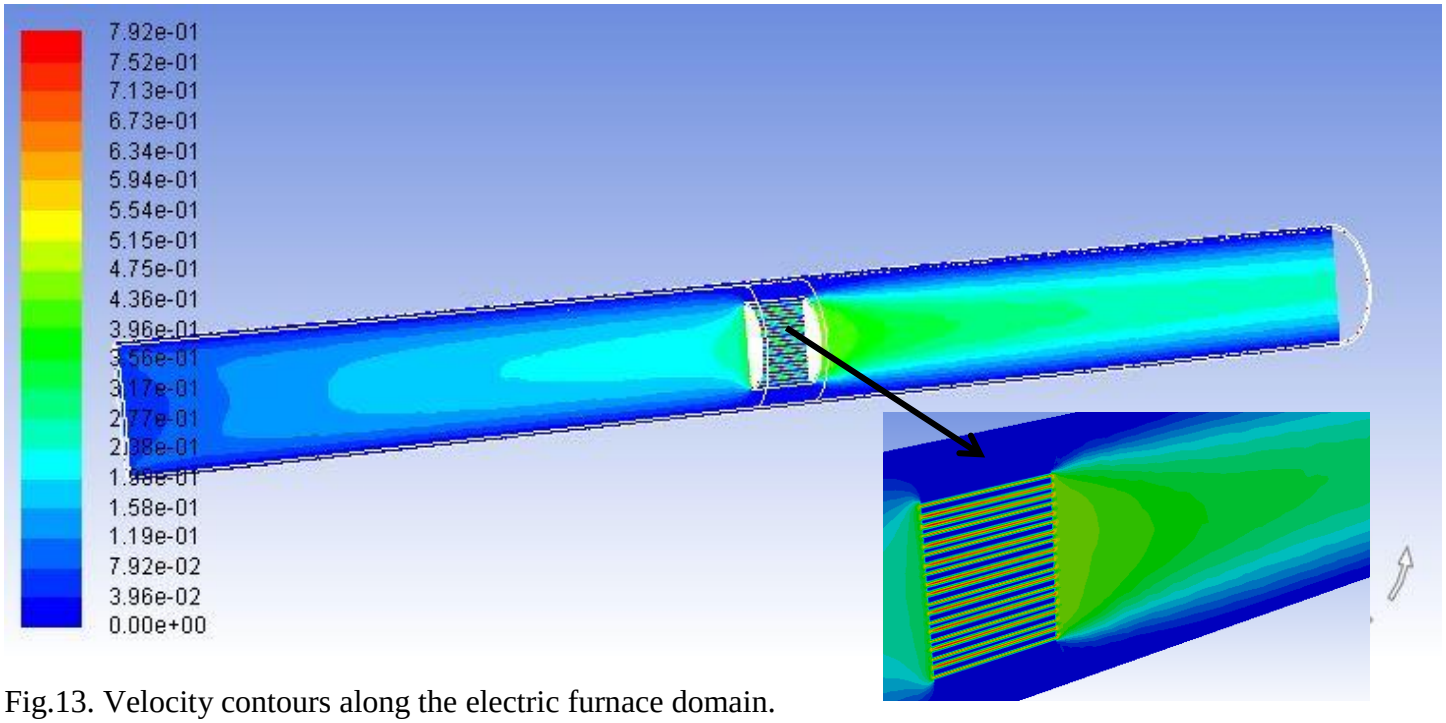

Fig.13. Velocity contours along the electric furnace domain.

The methane consumption is presented in Fig.14-a indicating the position of combustion. One of the combustion products CO_2 is shown in Fig.14-b. The concentration of CO is found to be less than 3 ppm at reactor outlet giving great agreement to the measurements obtained by experimental data by [25].

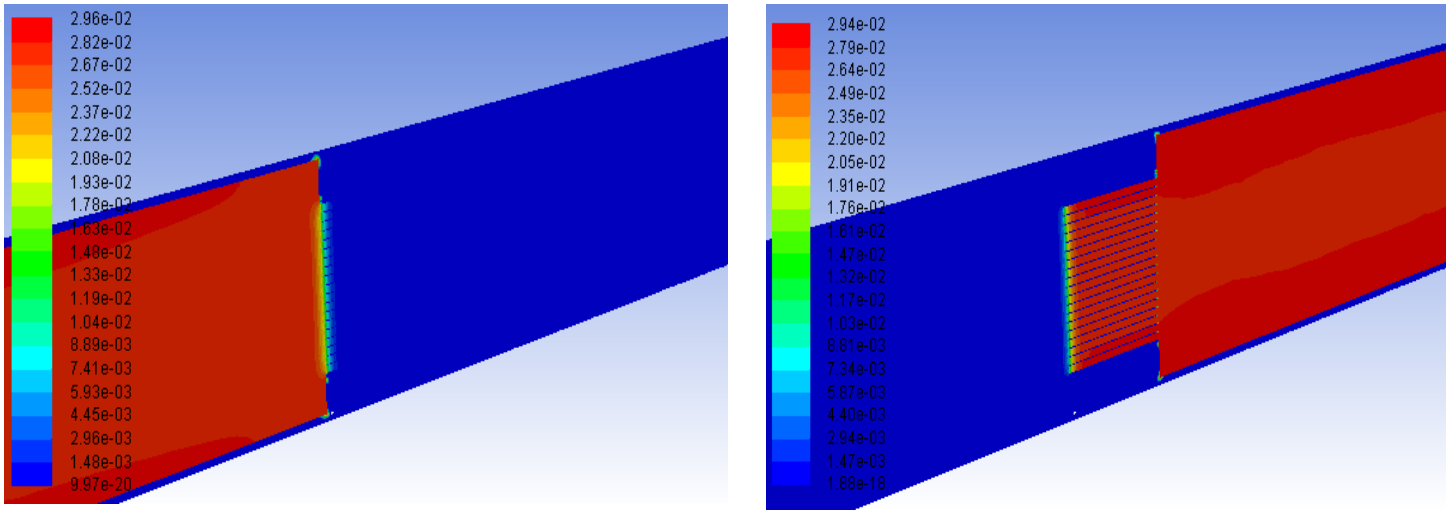

(a) CH_4 (b) CO_2

Fig.14. Contours of CH_4 and CO_2 mole fractions along the electric furnace domain.

3.3 Unsteady/transient operation

Under transient conditions, the combustion inside a micro tube burner is simulated adiabatically. The simulation was made by time step of 1.0 micro second for a micro tube burner having 0.85 mm diameter and 11 mm length with 40,000 total numbers of cells within the mesh domain. The flame front is noticed to move from upstream to downstream due to catalyst action at the surface. One shot at the end of the combustion process is shown in Fig.15.

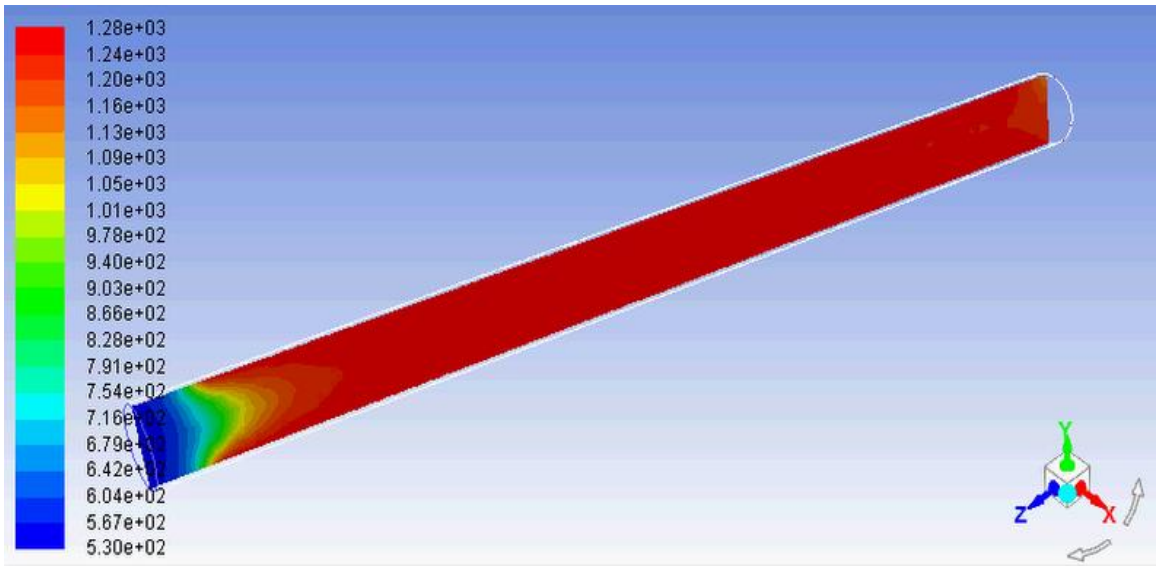

Fig.15. Temperature (K) contours inside the micro tube after combustion completion.

This behavior was previously observed in experimental work done by [29]. After achieving steady conditions, the flame front is located at one third of the tube length and and the remaining length attained equilibrium conditions. Simulation of the real experimental case was also done under transient conditions. The reaction front is clearly moving from upstream to downstream. The stable location of self-ignition depends upon the position (internally or externally) of the micro-burner which strongly governs the relation between heat losses and heat generation from combustion. Cimino and Di Benedetto [29] deduced experimentally that the reaction front moves backwards with temperature profiles shifting their maximum from the outlet section to the inlet section as shown in Fig.16. Also, it was declared that at steady state conditions, methane is almost completely converted in the first zone and the whole remaining zone operates as a heat provider.

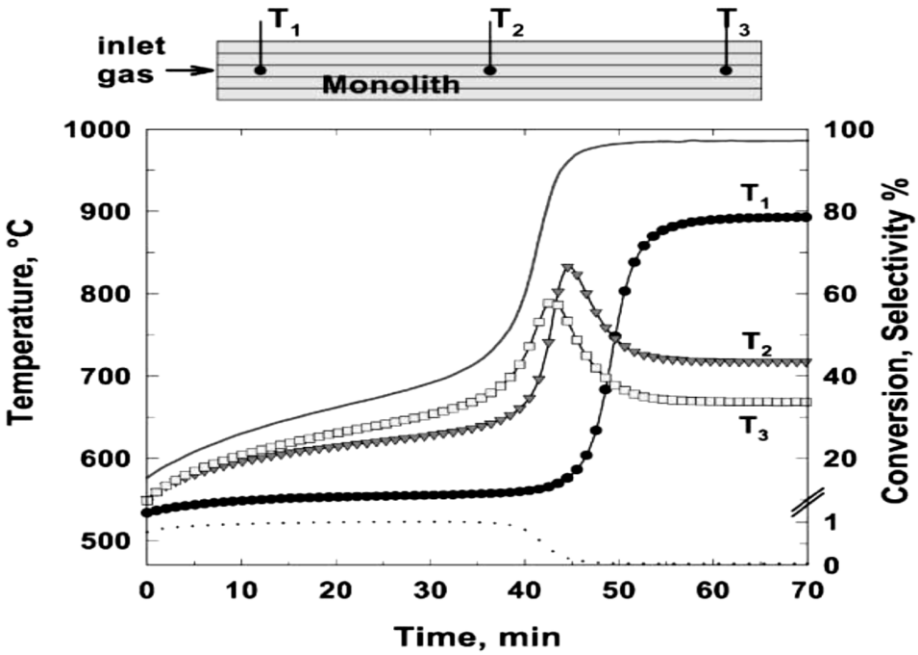

Fig.16. Transient temperature profiles reported experimentally by Cimino and Di Benedetto [29].

The simulation was made by time step of 1.0 micro second for the half of the reactor (axisymmetric) with 3 million mesh cells. The temperature contours at different time levels are presented in Fig.17 showing the progression of the auto-ignition within the reactor. It is observed that the reaction zone is apparently propagating from upstream to downstream which conforms qualitatively the experimental results of Fig. 16.

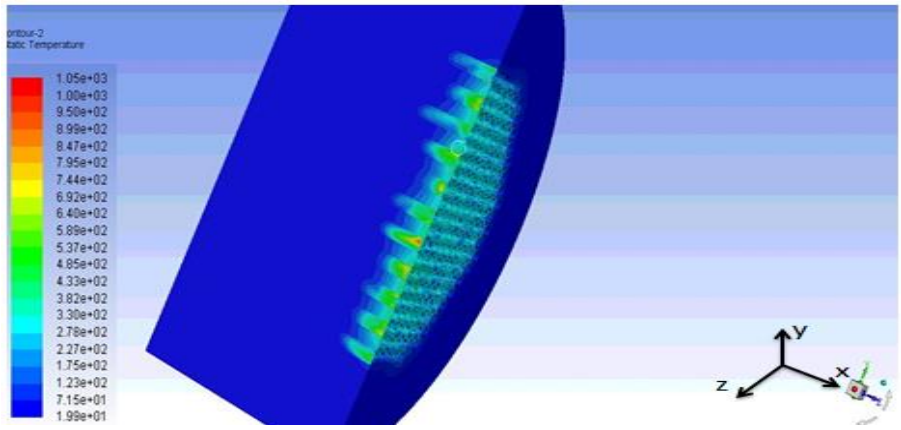

Fig.17. Temperature contours at about 0.5 second at a central cross-sectional plane of the reactor.

4. Conclusions

In this study, the auto-ignition characteristics over micro-structured catalytic honeycomb reactor for CH_4 and CH_4-H_2 mixtures have been investigated. Coupling of heat transfer and combustion in such micro-burner under pseudo-auto-thermal steady state conditions and transient cases, have been investigated using ANSYS 17.2 commercial package. A detailed CHEMKIN reaction kinetics mechanism has been considered for the calculations of species concentrations and reaction rates. Numerical validation of the minimum ignition temperature (*MIT*) results of CH_4-air mixtures has been performed utilizing the available data in the literature of a similar rector design. The effect of flow rate on the *MIT* of CH_4-air mixtures has been investigated. The effect of hydrogen-enrichment on the *MIT* of CH_4-air mixtures has also been investigated. It has been observed that addition of H_2 to CH_4 promotes the kinetics mechanism and advances the auto-ignition temperature by about 30 ˚C. The results showed that the ignition occurs at the same temperature for different mass flow rates of CH_4-air mixtures. However, for CH_4-H_2-air mixtures, the ignition temperature decreased while increasing

the flow rate. The flammability limits of methane-combustion in a micro catalytic reactor has been determined under lean mixture condition (equivalence ratio from 0.45 up to 0.75). The result have indicated new operating limits for methane-combustion in micro catalytic reactors that were not reported experimentally before. Under transient conditions, it has been noticed that the reaction front is clearly moving from upstream to downstream resembling the reported experimental behavior.

Acknowledgement

The authors like to appreciate the support received from King Fahd University of Petroleum and Minerals (KFUPM) to perform this work through the deanship of research on project number IN171018. The computational simulations were performed at Cairo University based on a collaboration agreement between all authors.

Compliance with Ethical Standards:

Funding: This study was funded by King Fahd University of Petroleum and Minerals (grant number IN171018).
Conflict of Interest: The authors declare that they have no conflict of interest.

References:

[1] YunFei Yan; Ying Liu; Haojie Li; Weipeng Huang; Yanrong Chen; Lixian Li; Zhongqing Yang. Effect of cavity coupling factors of opposed counter-flow micro-combustor on the methane-fueled catalytic combustion characteristics. J. Energy Resour. Technol. 2018; JERT-18-1199.

[2] Vidyasagar Shilapuram; Bishwadeep Bagchi; Nesrin Ozalp; Richard Davis. Statistical Modeling of Hydrogen Production Via Carbonaceous Catalytic Methane Decomposition. J. Energy Resour. Technol. 2018; 140(7):072006-072006-8.

[3] Omid Askari; Mimmo Elia; Matthew Ferrari; Hameed Metghalchi. Auto-Ignition Characteristics Study of Gas-to-Liquid Fuel at High Pressures and Low Temperatures. J. Energy Resour. Technol. 2016; 139(1):012204-012204-6.

[4] German Amador; Jorge Duarte Forero; Adriana Rincon; Armando Fontalvo; Antonio Bula; Ricardo Vasquez Padilla; Wilman Orozco. Characteristics of Auto-Ignition in Internal Combustion Engines Operated With Gaseous Fuels of Variable Methane Number. J. Energy Resour. Technol. 2017; 139(4):042205-042205-8.

[5] Ju Y, Maruta K. Microscale combustion: Technology development and fundamental research. Progress in Energy and Combustion Science 2011;37(6): 669-715.

[6] Daou J, Matalon M. Influence of conductive heat-losses on the propagation of premixed flames in channels. Combustion and Flame 2002;39:128-321.

[7] J Daou, M Matalon, " Flame propagation in Poiseuille flow under adiabatic conditions," Combustion and Flame,vol.49, pp.124-337, 2001.

[8] Ju Y, Xu B. Effects of channel width and Lewis number on the multiple flame regimes and propagation limits in mesoscale. Combustion Science and Technology 2006;53:178-189.

[9] Jackson TL, Buckmaster J, Lu Z, Kyritsis DC, Massa L. Flames in narrow circular tubes. Proceedings of the Combustion Institute 2007;31(1):955-962.

[10] Hua J, Wu M, Kumar K. Numerical simulation of the combustion of hydrogen–air mixture in micro-scaled chambers. Chemical Engineering Science 2005;60:3497–3506.

[11] Norton DG, Vlachos DG. Combustion characteristics and flame stability at the microscale: a CFD study of premixed methane/air mixtures. Chemical Engineering Science 2003;58:4871–4882.

[12] Li J, Choua SK. A numerical study on premixed micro-combustion of CH_4–air mixture:Effects of combustor size, geometry and boundary conditions on flame temperature. Chemical Engineering Science 2009;150:213–222.

[13] Karagiannidis S, Mantzaras J, Jackson G. Hetero-/homogeneous combustion and stability maps in methane-fueled catalytic micro reactors. Proceedings of the Combustion Institute 2007;31:3309-3317.

[14] Tang A, Xu Y, Pan J. A comparative study on combustion characteristics of methane, propane and hydrogen fuels in a micro-combustor. International Journal of Hydrogen Energy 2015;40:16587–16596.
[15] Tang A, Xu Y, Pan J. Combustion characteristics and performance evaluation of premixed methane/air with hydrogen addition in amicro-planar combustor. Chemical Engineering Science 2015;131:235–242.
[16] Shabanian SR, Sayed Reza. CFD Study on Hydrogen-Air Premixed Combustion in a Micro Scale Chamber. Iran. J. Chem. Chem. Eng. 2010;29(4).
[17] Li J, Choua SK. Study on premixed combustion in cylindrical micro combustors: Transient flame behavior and wall heat flux. Experimental Thermal and Fluid Science 2009;33:764–773.
[18] Sui R, Mantzaras J, Bombach R. Hetero-/homogeneous combustion of fuel-lean methane/ oxygen/nitrogen mixtures over rhodium at pressures up to 12 bar. Proceedings of the Combustion Institute 2017;36:4321-4328.
[19] Xu B, Ju Y. Concentration slip and its impact on heterogeneous combustion in a micro scale chemical reactor. Chemical Engineering Science 2005;72:60-73.
[20] Xu B, Ju Y. Theoretical and numerical studies of non-equilibrium slip effects on a catalytic surface. Combustion Theory and Modelling 2006;79:10-16.
[21] Aghalayam P, Bui PA, Vlachos DG. The role of radical wall quenching in flame stability and wall heat flux: hydrogen-air mixtures. Combustion Theory and Modelling 1998;30:2-6.
[22] Norton DG., Vlachos DG. Hydrogen-assisted self-ignition of propane/air mixtures in catalytic micro-burners. Proceedings of the combustion Institute 2005;30:473-2430.
[23] Sui R, Mantzaras J, Bombach R. Homogeneous ignition during fuel-rich $H_2/O_2/N_2$ combustion in platinum-coated channels at elevated pressures. Combustion and Flame 2017;180:184-195.
[24] Chen J, Xu D. Transient simulation of the hydrogen-assisted self-ignition of fuel-lean propane-air mixtures in platinum-coated micro-channels using reduced-order kinetics. Journal of Chemical Technology and Metallurgy 2016;51:90–98.
[25] Barbato PS, Landi G., Pirone R, Russo G, Scarpa A. Auto-thermal combustion of CH_4 and CH_4–H_2 mixtures over bi-functional Pt-$LaMnO_3$ catalytic honeycomb. Catalysis Today 2009;147S:271-278.
[26] Zimont VL. Theoretical study of self-ignition and quenching limits in a catalytic micro-structured burner and their sensitivity analysis. Chemical Engineering Science 2015;134:800-812.
[27] Semenov NN. Zur Theorie des Verbrennungsprozesses Z. Angew. Phys. 1928;48 (7-8):571-582.
[28] Zel'dovich YB, Barenblatt GI, Librovich VB, Machviladze GM. The Mathematical Theory of Combustion and Explosions Plenum Publishing Corporation, New York 1985.
[29] Cimino S, Di-Benedetto A. Transient behaviour of perovskite-based monolithic reactors in the catalytic combustion of methane. Catalysis Today 2001;69:95-103.
[30] Tang A, Deng J, Xu Y, Pan J, Cai T. Experimental and numerical study of premixed propane/air combustion in the micro-planar combustor with a cross-plate insert. Applied Thermal Engineering 2018;136:177-184.
[31] Deutschmann O, Schmidt R, Behrendt F, Wamat J. Numerical Modeling of Catalytic Ignition. Sym. (Int.) Combust. 1996;26:1747-1754.
[32] Boehman A. Radiation heat transfer in catalytic monoliths. AIChE J 1998;44:2745-1755.
[33] Dogwiler U, Mantzaras J, Benz P. Two-Dimensional Modelling for Catalytically Stabilized Combustion of a Lean Methane-Air Mixture With Elementary Homogeneous and Heterogeneous Chemical Reactions. Combustion and Flame 1999;116:243-258.
[34] Reinke M, Mantzaras J, Bombach R. Gas phase chemistry in catalytic combustion of methane/air mixtures over platinum at pressures of 1 to 16 bar. Combustion and Flame 2005;141:448-468.
[35] ANSYS Chemkin-Pro Theory Manual 17.2, ANSYS, Inc.: San Diego, 2016.